第29卷第2期 高能物理与核物理 Vol.29, No.2
2005年2月 HIGH ENERGY PHYSICS AND NUCLEAR PHYSICS Feb., 2005

High Spin States and Shape Coexistence in ^{134}Ce*

ZHU Sheng-Jiang[1;1)] GAN Cui-Yun[1] ZHU Ling-Yan[1] M. Sakhaee[1] YANG Li-Ming[1]
LONG Gui-Lu[1] WEN Shu-Xian[2] WU Xiao-Guang[2] LI Guang-Sheng[2] ZHU Li-Hua[2]
1 (Department of Physics, Tsinghua University, Beijing 100084, China)
2 (China Institute of Atomic Energy, Beijing 102413, China)

Abstract High spin states in ^{134}Ce nucleus have been studied by using the heavy-ion induced reaction ^{122}Sn(^{16}O,4n) carried out at China Institute of Atomic Energy. The early level scheme has been extended with spin up to 22$\hbar$. However, our result is different from that in a recent publication, and the magnetic rotation bands reported there have not been confirmed. Our observed level structures may be interpreted as shape coexistence. The 10^+ state at the backbending with $h_{11/2}$ quasineutron configuration has an oblate deformation with an asymmetry parameter $\gamma \approx -60°$ (Lund convention), and the 10^+ isomer is a yrast trap of prolate deformation with $\gamma \approx -120°$, whereas the other signature partner bands with $h_{11/2}$ and $g_{7/2}$ proton configuration probably have a prolate deformation with $\gamma \approx 0°$.

Key words nuclear structure, high spin states, shape coexistence

1 Introduction

The ^{134}Ce nucleus with $Z = 58$, $N = 76$ is located in the $A = 135$ deficient-neutron mass region. In this transitional region the nuclei are soft with respect to γ-value. The proton Fermi surface lies in the bottom of the $h_{11/2}$ subshell, while the neutron Fermi surface lies in the top of $h_{11/2}$ subshell. Cranked shell model (CSM) calculations[1] suggest that particles in the lower part of the $h_{11/2}$ subshell favor a collective prolate shape ($\gamma \approx 0°$ in the Lund convention[2]) or a triaxial shape ($\gamma \approx 30°$), while those in the upper midshell of the $h_{11/2}$ subshell favor a collective oblate shape ($\gamma \approx -60°$). Therefore, different configurations of the quasiparticles can drive a nucleus to form different shapes. In some nuclei, the shape coexistence can be observed, for example, in ^{132}Ba[3]. In previous publications, many rotational prolate and oblate bands as well as triaxial bands have been reported in Ce isotones, such as, in ^{132}Ce[4], ^{133}Ce[5,6], ^{135}Ce[7], ^{136}Ce[8], ^{137}Ce[9] and ^{138}Ce[10].

Study of the high spin states of ^{134}Ce can provide valuable information for the nuclear structure, the systematical shape change, the shape coexistence and the deformation driving effects of the single particle orbitals. In the early works, the low excited states of ^{134}Ce have been investigated by means of the β-decay of ^{134}Pr[11,12] and the high spin states have been reported by several groups using Ba(α, xn) reaction[13,14] and heavy ion reactions[15—18], including observing the superdeformation bands[17]. For the normal excitation states in ^{134}Ce, the highest spin state was observed with spin up to 18^+, and a 10^+ isomer was observed. However, comparing with the neighboring nuclei, the experimental data in ^{134}Ce is not sufficient as limited of the experimental techniques in the early work. Here we present the new high spin states of ^{134}Ce obtained by using the heavy ion reaction. The levels have been significantly extended and some new collective bands have been observed. A shape coexistence with different γ-values is suggested. As this work is finished, a new result of the magnetic rotation in ^{134}Ce has been reported in a recent publication[19]. However, we can not confirm the magnetic rotation bands in ^{134}Ce reported in Ref. [19].

Received 22 June 2004
* Supported by Major State Basic Research Development Program (G2000077405), National Natural Science Foundation of China (10375032), Special Program of Higher Education Science Foundation (20030003090)
1) E-mail: zhushj@mail.tsinghua.edu.cn

2 Experimental methods

The ^{122}Sn(^{16}O,4n) heavy-ion fusion-evaporation reaction was used to investigate high spin states of ^{134}Ce. An isotopically enriched ^{122}Sn target of 2.4mg/cm^2 evaporated on a natural lead backing of 19mg/cm^2 was used and bombarded by beam of ^{18}O ions accelerated by the HI-13 accelerator at China Institute of Atomic Energy (CIAE). The beam energy is 73MeV. An array of ten Compton-suppressed Ge detectors was employed to record γ-γ coincidence data. The resolutions of the Ge detectors are between 1.8—2.2keV at 1.333MeV γ-ray energy. The relative excitation function measurements, carried out using beam energies of 70, 73, 75 and 80MeV, were used to identify the γ-rays from the (^{16}O,3n), (^{16}O,4n) and (^{16}O,5n) reactions respectively. Approximately 170 × 10^6 coincidence events were collected, from which a γ-γ coincidence matrix was built. In order to determine the multipolarity of γ-ray transitions, four detectors at 90° with respect to the beam axis were sorted against the other six detectors (at 42°, 45°, 53°, 137°, 139° and 140°) to build a two-dimensional angular correlation matrix from which it was possible to ex-

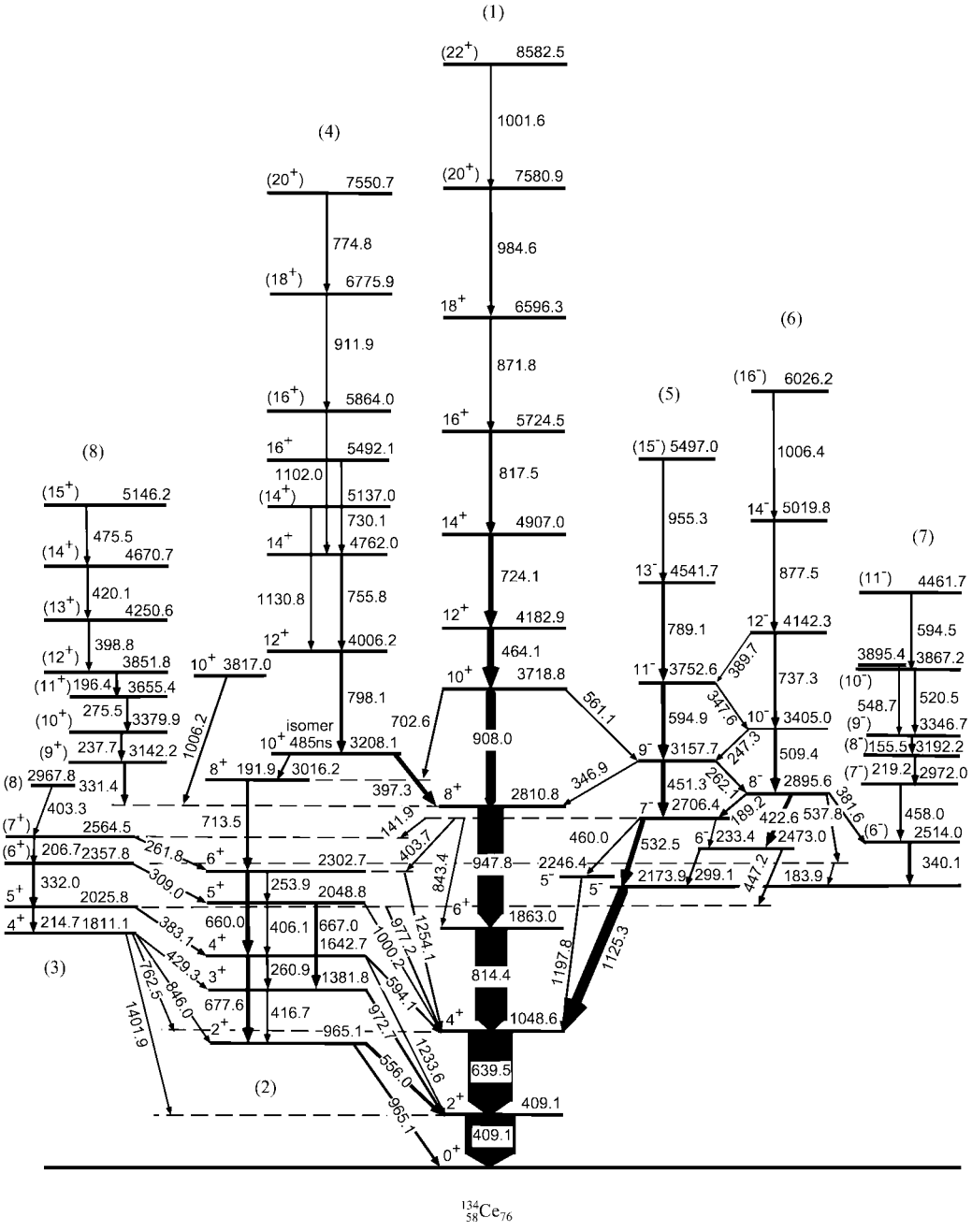

Fig. 1. Level scheme in ^{134}Ce.

tract average directional correlation of oriented state (DCO) intensity ratios. The γ-γ coincidence data were analyzed with the Radware software package[20].

3 Results

The level scheme of ^{134}Ce, deduced from the present study, is shown in Fig.1. It was constructed from γ-γ coincidence relations, relative transition intensities and DCO ratio analyzing. The collective bands or cascade structures are labeled on top or bottom of the scheme. The γ-rays attributed to ^{134}Ce in this experiment, together with the relative intensities of transitions, the DCO ratios, the γ-transition multiples, and the assignments of spin and parity (I^{π}) values are presented in Table 1. All the new transitions obtained in the present work are marked with an asterisk in the table. As examples, Fig.2 shows two spectra obtained by gating on 594.9keV transition in band (5) and 737.3keV one in band (6) respectively. In each spectrum, one can see corresponding coincidence γ-peaks observed in this experiment.

Table 1. Energies, intensities, and DCO data for the transitions assigned to ^{134}Ce.

E_γ/keV	E_i/keV	E_f/keV	Assignment	I/(%)	DCO ratio	Mult
141.9	2706.4	2564.5	$7^-\rightarrow(7^+)$	0.5		(E1)
*155.5	3346.7	3191.2	$(9^-)\rightarrow(8^-)$	0.8	1.42(18)	(M1/E2)
183.9	2357.8	2173.9	$(6^+)\rightarrow5^-$	0.8	1.27(17)	(E1)
189.2	2895.6	2706.4	$8^-\rightarrow7^-$	2.1	2.00(14)	M1/E2
191.9	3208.1	3016.2	$10^+\rightarrow8^+$	2.0	0.86(6)	E2
196.4	3851.8	3655.4	$(12^+)\rightarrow(11^+)$	1.4	1.13(7)	(M1)
206.7	2564.5	2357.8	$(7^+)\rightarrow(6^+)$	2.1	1.36(7)	(M1/E2)
214.7	2025.8	1811.1	$5^+\rightarrow4^+$	3.1	1.40(7)	M1/E2
*219.2	3191.2	2972.0	$(8^-)\rightarrow(7^-)$	1.4	1.38(13)	(M1/E2)
233.4	2706.4	2473.0	$7^-\rightarrow6^-$	0.7		M1/E2
237.7	3379.9	3142.2	$(10^+)\rightarrow(9^+)$	3.0	1.13(7)	(M1/E2)
*247.3	3405.0	3157.7	$10^-\rightarrow9^-$	0.4		M1/E2
253.9	2302.7	2048.8	$6^+\rightarrow5^+$	<0.4		M1/E2
260.9	1642.7	1381.8	$4^+\rightarrow3^+$	1.4	1.33(7)	M1/E2
261.8	2564.5	2302.7	$7^+\rightarrow6^+$	1.7	1.32(8)	M1/E2
262.1	3157.7	2895.6	$9^-\rightarrow8^-$	3.3	1.48(14)	M1/E2
275.5	3655.4	3379.9	$(11^+)\rightarrow(10^+)$	2.0	1.05(8)	(M1)
299.1	2473.0	2173.9	$6^-\rightarrow5^-$	4.9	1.61(6)	M1/E2
309.0	2357.8	2048.8	$(6^+)\rightarrow5^+$	3.0	1.14(8)	(M1/E2)
331.4	3142.2	2810.8	$(9^+)\rightarrow8^+$	3.4	1.12(8)	(M1/E2)
332.0	2357.8	2025.8	$(6^+)\rightarrow5^+$	1.5		(M1/E2)
*340.1	2514.0	2173.9	$(6^-)\rightarrow5^-$	1.9	1.31(14)	(M1/E2)
346.9	3157.7	2810.8	$9^-\rightarrow8^+$	0.9	1.49(9)	E1
*347.6	3752.6	3405.0	$11^-\rightarrow10^-$	1.6		M1/E2
381.6	2895.6	2514.0	$8^-\rightarrow(6^-)$	<0.4		(E2)
383.1	2025.8	1642.7	$5^+\rightarrow4^+$	2.2	1.10(10)	M1/E2
*389.7	4142.3	3752.6	$12^-\rightarrow11^-$	<0.4		M1/E2
397.3	3208.1	2810.8	$10^+\rightarrow8^+$	14.0	0.82(3)	E2
*398.8	4250.6	3851.8	$(13^+)\rightarrow(12^+)$	1.3	1.23(10)	(M1/E2)
403.3	2967.8	2564.5	$(8)\rightarrow7^+$	2.0	1.46(9)	
403.7	2706.4	2302.7	$7^-\rightarrow6^+$	2.0	1.44(8)	E1
406.1	2048.8	1642.7	$5^+\rightarrow4^+$	0.9		M1/E2
409.1	409.1	0	$2^+\rightarrow0^+$	100	0.81(3)	E2
416.7	1381.8	965.1	$3^+\rightarrow2^+$	1.9	1.72(10)	M1/E2

Table 1 continued

E_γ/keV	E_i/keV	E_f/keV	Assignment	I/(%)	DCO ratio	Mult
*420.1	4670.7	4250.6	$(14^+)\rightarrow(13^+)$	0.9	1.23(10)	(M1/E2)
422.6	2895.6	2473.0	$8^-\rightarrow6^-$	8.5	0.79(8)	E2
429.3	1811.1	1381.8	$4^+\rightarrow3^+$	0.9	1.60(10)	M1/E2
447.2	2473.0	2025.8	$6^-\rightarrow(5^+)$	4.3		(E1)
451.3	3157.7	2706.4	$9^-\rightarrow7^-$	10.6	0.66(6)	E2
*458.0	2972.0	2514.0	$(7^-)\rightarrow(6^-)$	1.6	1.50(20)	(M1/E2)
*460.0	2706.4	2246.4	$7^-\rightarrow5^-$	1.5		E2
464.1	4182.9	3718.8	$12^+\rightarrow10^+$	16.9	0.81(4)	E2
*475.5	5146.2	4670.7	$(15^+)\rightarrow(14^+)$	0.6		(M1/E2)
*509.4	3405.0	2895.6	$10^-\rightarrow8^-$	7.8	0.79(9)	E2
*520.5	3867.2	3346.7	$(10^-)\rightarrow(9^-)$	0.8		(M1/E2)
532.5	2706.4	2173.9	$7^-\rightarrow5^-$	13.7	0.72(6)	E2
537.8	2895.6	2357.8	$8^-\rightarrow(6^+)$	3.4		(M2)
*548.7	3895.4	3346.7	$\rightarrow(9^-)$	0.6		
556.0	965.1	409.1	$2^+\rightarrow2^+$	9.0	0.78(5)	E2
*561.1	3718.8	3157.7	$10^+\rightarrow9^-$	1.7		E1
594.1	1642.7	1048.6	$4^+\rightarrow4^+$	4.8	0.85(4)	E2
*594.5	4461.7	3867.2	$(11^-)\rightarrow(10^-)$	0.6		(M1/E2)
594.9	3752.6	3157.7	$11^-\rightarrow9^-$	10.8	0.79(8)	E2
639.5	1048.6	409.1	$4^+\rightarrow2^+$	93.8	0.83(2)	E2
660.0	2302.7	1642.7	$6^+\rightarrow4^+$	9.8	0.77(5)	E2
667.0	2048.8	1381.8	$5^+\rightarrow3^+$	8.4	0.73(5)	E2
677.6	1642.7	965.1	$4^+\rightarrow2^+$	11.3	0.79(5)	E2
702.6	3718.8	3016.2	$10^+\rightarrow8^+$	3.5	0.79(10)	E2
713.5	3016.2	2302.7	$8^+\rightarrow6^+$	6.9	0.73(6)	E2
724.1	4907.0	4182.9	$14^+\rightarrow12^+$	14.2	0.89(5)	E2
730.1	5492.1	4762.0	$16^+\rightarrow14^+$	2.1	0.59(6)	E2
*737.3	4142.3	3405.0	$12^-\rightarrow10^-$	4.7	0.87(12)	E2
755.8	4762.0	4006.2	$14^+\rightarrow12^+$	4.6	0.88(6)	E2
762.5	1811.1	1048.6	$4^+\rightarrow4^+$	1.8	0.81(6)	E2
*774.8	7550.7	6775.9	$(20^+)\rightarrow(18^+)$	<0.4		(E2)
789.1	4541.7	3752.6	$13^-\rightarrow11^-$	7.0	0.79(10)	E2
798.1	4006.2	3208.1	$12^+\rightarrow10^+$	7.4	0.83(5)	E2
814.4	1863.0	1048.6	$6^+\rightarrow4^+$	57.0	0.83(3)	E2
817.5	5724.5	4907.0	$16^+\rightarrow14^+$	7.0	0.84(7)	E2
*843.4	2706.4	1863.0	$7^-\rightarrow6^+$	2.1		E1
846.0	1811.1	965.1	$4^+\rightarrow2^+$	1.2	0.72(5)	E2
871.8	6596.3	5724.5	$18^+\rightarrow16^+$	5.3	0.89(7)	E2
*877.5	5019.8	4142.3	$14^-\rightarrow12^-$	2.6	0.87(10)	E2
908.0	3718.8	2810.8	$10^+\rightarrow8^+$	21.8	0.98(4)	E2
*911.9	6775.9	5864.0	$(18^+)\rightarrow(16^+)$	0.7		(E2)
947.8	2810.8	1863.0	$8^+\rightarrow6^+$	47.5	0.89(2)	E2
955.3	5497.0	4541.7	$(15^-)\rightarrow13^-$	2.2		(E2)
965.1	965.1	0	$2^+\rightarrow0^+$	8.7		E2
972.7	1381.8	409.1	$3^+\rightarrow2^+$	7.0	1.07(7)	M1/E2
977.2	2025.8	1048.6	$5^+\rightarrow4^+$	2.8		M1

Table 1 continued

E_γ/keV	E_i/keV	E_f/keV	Assignment	I/(%)	DCO ratio	Mult
*984.6	7580.9	6596.3	$(20^+)\rightarrow 18^+$	2.2		(E2)
1000.2	2048.8	1048.6	$5^+\rightarrow 4^+$	2.1		(M1/E2)
*1001.6	8582.5	7580.9	$(22^+)\rightarrow 20^+$	1.5		(E2)
*1006.2	3817.0	2810.8	$10^+\rightarrow 8^+$	3.2	0.77(7)	E2
*1006.4	6026.2	5019.8	$(16^-)\rightarrow 14^-$	1.2		(E2)
*1102.0	5864.0	4762.0	$(16^+)\rightarrow 14^+$	1.4		(E2)
1125.3	2173.9	1048.6	$5^-\rightarrow 4^+$	28.7	1.56(4)	E1
*1130.8	5137.0	4006.2	$(14^+)\rightarrow 12^+$	0.7		(E2)
1197.8	2246.4	1048.6	$5^-\rightarrow 4^+$	5.3	1.36(10)	E1
1233.6	1642.7	409.1	$4^+\rightarrow 2^+$	2.0	0.89(12)	E2
1254.1	2302.7	1048.6	$6^+\rightarrow 4^+$			E2
1402.0	1811.1	409.1	$4^+\rightarrow 2^+$			E2

* new transitions in the present work.

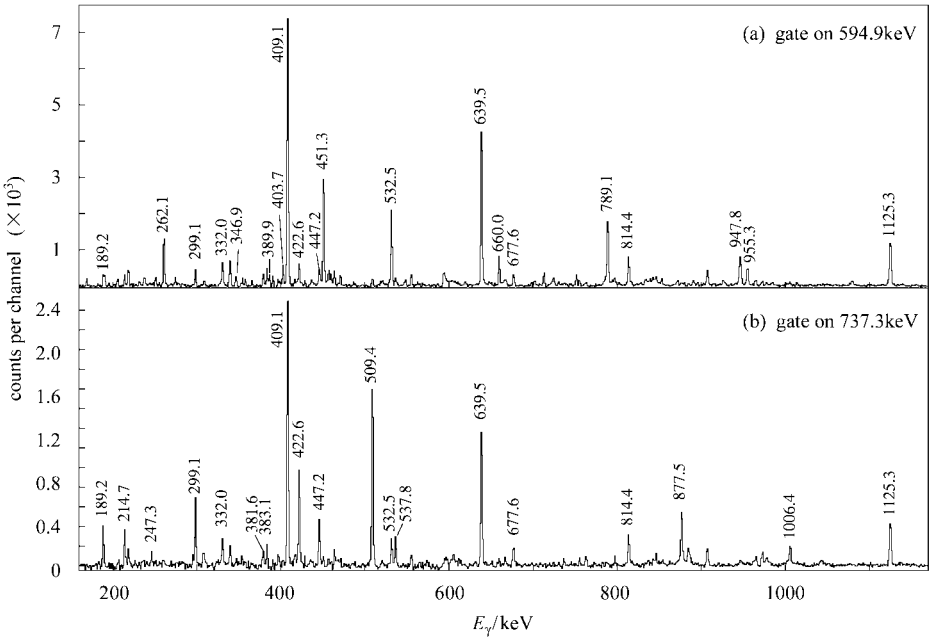

Fig.2. Coincidence spectra obtained by gating on (a) the 594.5keV γ-transition of band (5) and (b) the 737.3keV γ-transition of band (6).

Comparing our results with those in previous publications[13—17], the level scheme has been significantly updated and many new levels and transitions are discovered. The I^πs for the levels have been assigned or tentatively assigned based on the previous works[13—17] and the DCO ratio values measured in this work. The band (1) has been extended with spin up to 22ħ. Two new levels at 7580.9 and 8582.5keV, along with 984.6 and 1001.6keV transitions were added above the 18^+ state. At the lower excited states, a new transition 406.1keV ($5^+\rightarrow 4^+$) inside the band (2) was observed in this work. However, in this band, a level at 2767keV with $I^\pi = 7^+$ reported in Ref. [12], was not observed. Above the 10^+ state at 3208.1keV, some levels with E2 linking transitions have been observed as labeled as (4) in Fig.1. Among them, two levels at 4006.2 and 4762.0keV, along with 798.1 and 755.8keV linking transitions, reported in Ref. [14] are confirmed in this work. The 5492.1keV level and the 730.1keV transition with dashed lines in Ref. [14] are confirmed by our work also. Besides, four new levels at 5137.0, 5864.0, 6775.9 and 7550.7keV as well as the linking transi-

tions, 1130.8, 1102.0, 911.9 and 774.8keV have been observed. For the negative parity levels, we suggest that two collective bands (5) and (6) are based on 7^- level at 2706.4 keV and 8^- level at 2895.6keV respectively, according to the regular level spacings inside the each band. At the lower spins, the negative parity levels and the linking transitions above the 5^- level at 2173.9keV until the 9^- level at 3157.7 keV of band (5) and the 8^- level at 2895.6keV of band (6) previously reported in Refs. [14,18] have been confirmed by this work. Above the 9^- level of band (5), three levels at 3752.6, 4541.7 and 5497.0keV along with the 594.9, 789.1 and 955.3keV linking transitions, reported in Ref. [18] but not in Ref. [14], have been observed in this work. The band (6) based on the 8^- state is newly established with spin up to $16\hbar$. Three new crossover $\Delta I = 1$ transitions, 247.3, 347.6 and 389.7keV are observed, in addition to the two ones, 189.2 and 262.1keV reported in previous work[14]. At the right part of the Fig.1, above the 5^- level at 2173.9keV, seven new levels along with seven new linking transitions have been observed, as labeled as (7) in the scheme. We tentatively assign the levels as negative parity. For a cascade of the left part of the Fig.1, labeled as (8), the levels until to the 3851.8keV, as well as the linking transitions reported in Ref. [14] were confirmed in the present work. Above the 3851.8 keV level, a weak collective band has been newly observed.

However, our level scheme in ^{134}Ce observed in the present work is much different from that published in Ref. [19]. The two magnetic rotation bands have been reported in Ref. [19] but not in this work. We analyzed the data carefully and can not confirm the results of the two magnetic rotation bands B4 and B5 established in Ref. [19] (see Fig.1 in Ref. [19]). On the other hand, most of the transitions inside the bands B4 and B5 reported in Ref. [19] have been put in the cascades (8) and (7) of Fig.1 in the present work. They form two complex structures. Our assignments for these two cascades are based on the coincidence relationships of the γ-transitions as well as the transition intensity relationships (see Table 1). As examples, Figs.3 and 4 show two spectra obtained by gating on 196.4keV transition {in cascade (8) in Fig.1 or in band B4 in Fig.1 of Ref. [19]} and 219.2keV transition {in cascade (9) in Fig.1 or in band B5 in Fig.1 of Ref. [19]} respectively. One can see very strong coincidence γ-peaks, such as at 237.7, 275.5, 331.4, 398.8, 409.1, 420.1, 475.5, 639.5, 814.4 and 947.8keV in Fig.3 and at 155.5, 340.1, 409.1, 458.0, 520.5, 548.7, 594.5, 639.5, and 1125.3keV in Fig.4. But the coincidence linking transition peaks reported in Ref. [19] are very weak or invisible (the peaks are asterisked in Figs.3 and 4 respectively).

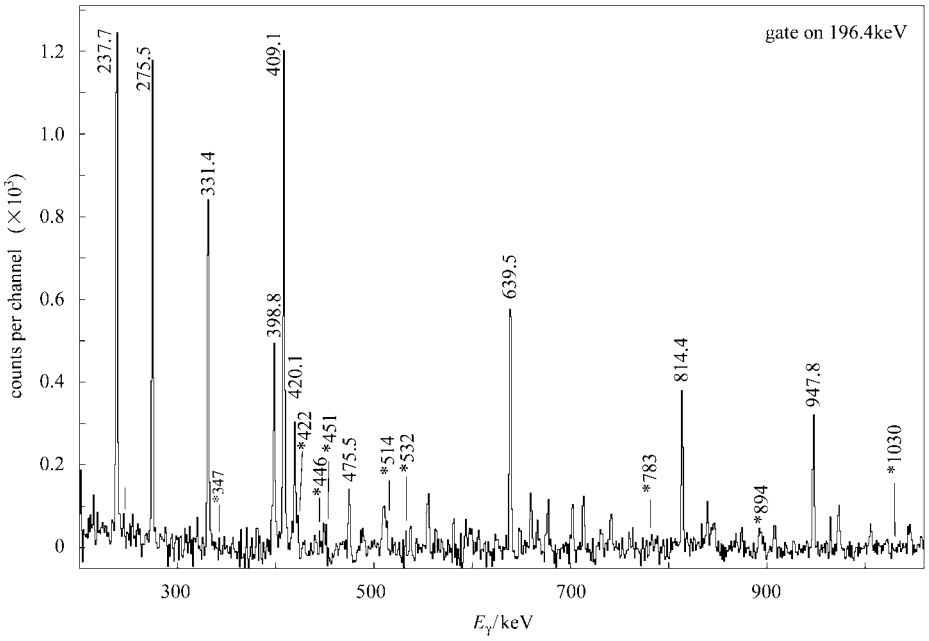

Fig.3. Coincidence spectra obtained by gating on 196.4keV γ-transition of cascade (8) in Fig.1 or band B4 in Ref. [19]. The asterisked peaks indicate the linking transitions from band B4 in Ref. [19].

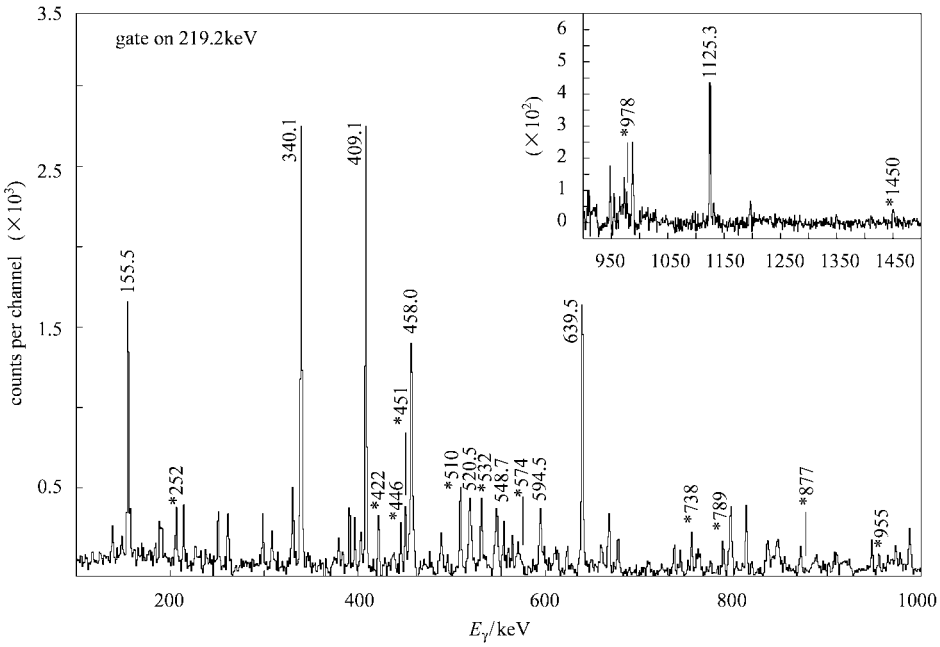

Fig.4. Coincidence spectra obtained by gating on 219.2keV γ-transition of cascade (7) in Fig.1 or band B5 in Ref. [19]. The asterisked peaks indicate the linking transitions in Ref. [19].

4 Discussion

The levels of ^{134}Ce exhibit complex characteristics. It has the high level density. Until the state up to 8^+ of the band (1), the level spacings have an $I(I+1)$ dependence and it belongs to ground state band or yrast band. The calculated $E(4_1^+)/E(2_1^+)$ ratio of 2.56 lies between the ratios 2.64 in ^{132}Ce[4] and 1.98 in ^{136}Ce[8]. It indicates that ^{134}Ce has more deformation than that in ^{136}Ce, but less than that in ^{132}Ce. Previously theoretical calculations[21—23] predict a shape of ^{134}Ce with $\gamma \approx -30°$ for the ground state band. Band (2) based on 965.1keV level (2^+ state) belongs a γ-band as reported in Refs.[12,14]. As the level spacings inside this band are more irregular than those in the normal γ-band, it was proposed as "quasi-γ-band". The irregularity of the level spacings may be caused by γ-deformation or γ-softness. The band (3) built on 1811.1keV level (4^+ state) was assigned as "$K=4^+$" band[12]. As the excitation energy of the band head is only 1811.1keV, it is not likely to be a quasi-particle excitation band. We assign it as "quasi-2γ-band".

Above the 8^+ state in the band (1), the structural variation happens and the levels become no-yrast ones. A second 10^+ level at 3208.1keV becomes yrast state. Fig.5 shows plots of the kinetic moments of inertia J_1 against the rotational frequencies $\hbar\omega$ for the band (1) in ^{134}Ce as well as the yrast bands in ^{130}Ce[24] and ^{132}Ce[4]. One can see the band crossing occurred with rotating frequencies at $\hbar\omega \approx 0.30, 0.40$ and 0.34MeV in ^{130}Ce, ^{132}Ce and ^{134}Ce respectively. Both the curves in ^{130}Ce and ^{132}Ce show the normal backbending. But the origination of the band cross for the two isotopes is different with an aligned pair of $h_{11/2}$ quasiprotons in ^{130}Ce[24] and $h_{11/2}$ quasineutrons in ^{132}Ce[4] respectively, according to the cranked shell model (CSM) calculations. On the other hand, observed backbending of ^{134}Ce is sharper than those in ^{130}Ce

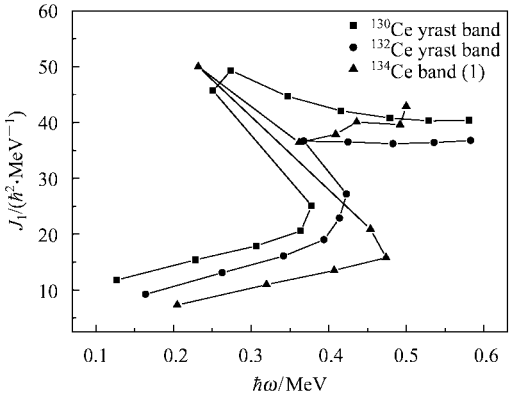

Fig.5. Plots of the kinetic moments of inertia J_1 against rotational frequencies $\hbar\omega$ for band (1) in ^{134}Ce, and yrast bands in ^{130}Ce[24] and ^{132}Ce[4].

and ^{132}Ce. Previous g-factor measurements[18] indicate that the 10^+ state in band (1) of ^{134}Ce has the configuration of $h_{11/2}$ neutrons. Meanwhile, the CSM calculations[14] indicate that the backbending in band (1) of ^{134}Ce is caused by an aligned pair of $h_{11/2}$ quasineutrons and the aligned band probably has an oblate deformation with $\gamma \approx -60°$.

The yrast 10^+ state at 3208.1keV is an isomer with a life-time 485 ns[14]. Above the 10^+ isomer, the level spacings are irregular and they show the single-particle excitation character. As discussed in Ref. [14], the 10^+ isomer in ^{134}Ce may have feature of an yrast trap. Considering the results of the g-factor measurements[18], it has been interpreted as $\nu[h_{11/2}]^2$ configuration also, as observed in ^{136}Ce[25]. Furthermore, the CSM calculations indicate that the 10^+ isomer has a γ-deformation of $-120°$[14] and belongs to a prolate deformation. Thus, both the 10^+ states in ^{134}Ce originate from $h_{11/2}$ two-quasineutron configurations, but the isomer corresponds to the lowest lying one[14].

Since the negative parity bands (5) and (6) are interconnected by $\Delta I = 1$ transitions, it is likely to be signature partners with $\alpha = 1$ for band (5) and $\alpha = 0$ for band (6) respectively. They form a strongly coupled band structure. Examining the structures of $N = 76$ neighboring even-even isotones, a similar signature partner structure has been observed in ^{132}Ba (see the bands (10) and (11) of the Fig.2 in Ref. [26]), and it has been suggested to respond to the proton $h_{11/2}$ and $g_{7/2}$ configuration. Based on the systematical comparison with ^{132}Ba, we propose that the signature partner bands (5) and (6) are originated from the proton $h_{11/2}$ and $g_{7/2}$ configuration ($\pi h_{11/2} \otimes \pi g_{7/2}$) also. This assignment is supported by the comparison of alignments of the angular moments with that in the ^{133}La nucleus[27]. The experimental alignments for the bands (5) and (6) of ^{134}Ce are presented in Fig.6, as a function of rotational frequency. The plots were produced using Harris parameters of $\mathcal{J}_0 = 5.0\hbar^2\text{MeV}^{-1}$ and $\mathcal{J}_1 = 53.8\hbar^4\ \text{MeV}^{-3}$[14]. The sum of alignments of the proton $h_{11/2}$ and $g_{7/2}$ bands in the ^{133}La[27] is much closed to that extracted in bands (5) and (6) in ^{134}Ce. On the other hand, the TRS calculations suggest that the two-quasiproton bands have a shape with a positive γ ($\gamma \approx 0°$—$30°$)[3]. For the two-quasiproton bands in ^{132}Ba a shape with $\gamma \approx 30°$ is suggested[26]. As the signature splitting of the bands (5) and (6) in ^{134}Ce is less than that in ^{132}Ba, we suggest that the two-quasiproton bands (5) and (6) in ^{134}Ce is with a shape with $\gamma \approx 0°$, a prolate deformation. The 5^- level at 21731.9 keV and the 6^- level at 2473.0keV below the bands (5) and (6) belong to single-particle excitation states, likely originated from the neutron configurations, $\nu h_{11/2} \otimes \nu s_{1/2}$ and $\nu h_{11/2} \otimes \nu d_{5/2}$ respectively[14].

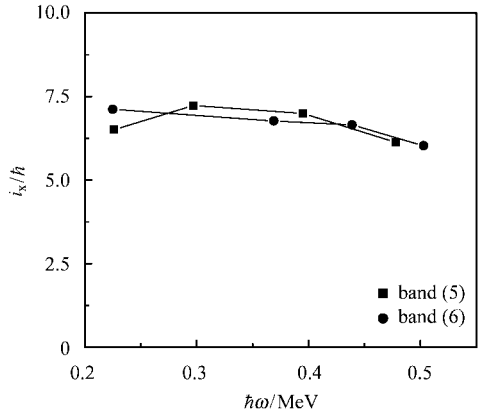

Fig.6. Experimental alignments for bands (5) and (6) of ^{134}Ce.

The cluster of negative parity levels (7) does not likely form a collective band structure as the irregularity of the level spacings. The levels may originate from the multi-quasineutron configurations. For the positive parity levels of the cascade (8), the origination for these single-particle levels and the weak collective band based on the 3655.4keV level are not clear. They may come from the multi-quasineutron configurations also. To make explanation for this complex structure, more experimental and theoretical work is needed.

5 Summary

High spin states of ^{134}Ce have been studied using ^{16}O-induced reactions at China Institute of Atomic Energy. The previously known levels and transitions have been confirmed and many new levels and transitions have been observed. The magnetic rotation bands reported in a recent publication can not be confirmed. The characteristics of the collective bands and the single-particle states, including the 1γ-2γ-bands, the ground state band, the backbending above the ground state band, the new signature partner bands and the isomer have been discussed. The observed three different structures may be interpreted as a shape coexistence with different γ-values. The 10^+ state above the ground state band with $h_{11/2}$ quasineutron configuration has an oblate deformation with an asymmetry parameter $\gamma \approx -60°$, and the 10^+ isomer, with $h_{11/2}$ quasineutron configuration too, is a yrast trap of prolate

deformation with $\gamma \approx -120°$, whereas the other two signature partner bands with $h_{11/2}$ and $g_{7/2}$ proton configuration probably has a prolate deformation with $\gamma \approx 0°$, according to the cranked shell model calculations.

References

1 Paul E S, Beausang C W et al. Phys. Rev. Lett., 1987, **58**: 984
2 Andersson G, Larsson S E, Leander G et al. Nucl. Phys., 1976, **A268**: 205
3 Paul E S, Fossan D B, Liang Y et al. Phys. Rev., 1989, **C40**: 1255
4 Paul E S, Boston A J, Joss D T et al. Nucl. Phys., 1999, **A619**: 177
5 Ma R, Paul E S, Beausang C W et al. Phys. Rev., 1987, **C36**: 2322
6 Hauschild K, Wadsworth R, Clark R M et al. Phys. Rev., 1986, **C54**: 613
7 Ma R, Paul E S, Fossan D B et al. Phys. Rev., 1990, **C41**, 2624
8 Paul E S, Fossan D B, Liang Y et al. Phys. Rev., 1990, **C41**: 1576
9 ZHU S J, ZHU L Y, LI M et al. Phys. Rev., 2000, **C62**: 044310
10 ZHU S J, LI M, ZHU L Y et al. Chin. Phys. Lett., 1999, **16**: 635
11 Arlt R, Beyer G, Fominykh V et al. Acta. Phys. Pol., 1973, **B4**: 301
12 Gade A, Wiedenhöver I, Luig M et al. Nucl. Phys., 2000, **A673**: 45
13 Smith G L, Draper J E. Phys. Rev., 1970, **C1**: 1548
14 Müller-Veggian M, Beuscher H, Haenni D R et al. Nucl. Phys., 1984, **A417**: 189
15 Ward D, Diamond R M, Stephens F S. Nucl. Phys., 1968, **A117**: 309
16 Goldberg M B, Broude C, Dafni E et al. Phys. Lett., 1980, **B97**: 351
17 O'Brien N J, Galindo-Uribarri A, Janzen V P et al. Phys. Rev., 1999, **C59**: 1334
18 Zemel A, Broude C, Dafni E et al. Nucl. Phys., 1982, **A383**: 165
19 Lakshmi S, Jain H C, Joshi P K et al. Phys. Rev., 2004, **C69**: 014319
20 Radford D C. Nucl. Instrum. Methods Phys. Res., 1995, **A361**: 297
21 Kern B D, Mlekodaj R L, Leander G A et al. Phys. Rev., 1987, **C36**: 1514
22 Wyss R, Nyberg J, Johnson A et al. Phys. Lett., 1988, **B215**: 211
23 Chen Y S, Frauendorf S, Leander G A. Phys. Rev., 1983, **C28**: 2437
24 Todd D M, Aryaeinejad R, Love D J G et al. J. Phys. G: Nucl. Phys., 1984, **10**: 1407
25 Müller-Veggian M, Gono Y, Lieder R M et al. Nucl. Phys., 1978, **A304**: 1
26 Juutinen S, Törmänen S, Ahonen P et al. Phys. Rev., 1995, **C52**: 2946
27 Hildingson L, Klamra W, Lindblad Th et al. Z. Phys., 1991, **A338**: 125

^{134}Ce 核的高自旋态与形状共存*

朱胜江[1;1)] 甘翠云[1] 朱凌燕[1] M.萨哈伊[1] 杨利明[1]
龙桂鲁[1] 温书贤[2] 吴晓光[2] 李广生[2] 竺礼华[2]

1(清华大学物理系 北京 100084)
2(中国原子能科学研究院 北京 102413)

摘要 在中国原子能科学研究院 H-13 串列加速器上,通过重离子核反应 ^{122}Sn(^{16}O,4n)对 $A = 130$ 缺中子核区的 ^{134}Ce 核的高自旋态进行了研究,建立了 ^{134}Ce 的新的能级纲图,最高自旋态扩展到 $22\hbar$. 然而实验结果与近期发表的 ^{134}Ce 核的高自旋态结果不同,所谓在 ^{134}Ce 核中存在的磁转动带结构不能被实验证实. 对实验结果的分析表明,^{134}Ce 核的高自旋态结构呈现出重要的形状共存特性:在基带以上的回弯处的 10^+ 态起源于两个中子组态,基于此 10^+ 态的转动带具有 $\gamma \approx -60°$ 的扁椭形变;另一个 10^+ 同质异能态为 yrast 陷阱,也起源于两中子组态,为具有 $\gamma \approx -120°$ 的长椭形状;而由两个 signature 伙伴带组成的强耦合带,则起源于 $h_{11/2}$ 与 $g_{7/2}$ 质子组态,为具有 $\gamma \approx 0°$ 的长椭形变带.

关键词 核结构 高自旋态 形状共存

2004-06-22 收稿

*国家重点基础研究发展规划项目(G2000077405),国家自然科学基金(10375032),教育部博士点基金(20030003090)资助

1) E-mail: zhushj@mail.tsinghua.edu.cn